Peptide-vector strategy bypasses P-glycoprotein efflux, and enhances brain transport and solubility of paclitaxel

Emmanuelle Blanc[a], Cécile Bonnafous[a], Peggy Merida[a], Salvatore Cisternino[b], Philippe Clair[c], Jean-Michel Scherrmann[b] and Jamal Temsamani[c]

We present the results obtained with paclitaxel coupled to a peptide-vector SynB3 (PAX-OSUC-SynB3), showing that this peptide-vector enhances the solubility of paclitaxel and its brain uptake in mice using the *in situ* brain perfusion model. We also show by the *in situ* brain perfusion in P-glycoprotein (P-gp)-deficient and wild-type mice that vectorized paclitaxel bypasses the P-gp present at the luminal side of the blood–brain barrier. The effect of the vectorized paclitaxel on various cancer cells was not significantly different from that of free paclitaxel. These results indicate that vectorization of paclitaxel may have significant potential for the treatment of brain tumors. *Anti-Cancer Drugs* 15:947–954 © 2004 Lippincott Williams & Wilkins.

Anti-Cancer Drugs 2004, **15**:947–954

Keywords: brain uptake, multidrug resistance, P-glycoprotein, paclitaxel, peptide conjugate, SynB vector

[a]Synt:em, Institut de Génétique Moléculaire de Montpellier, CNRS UMR 5535, Montpellier, France, [b]INSERM U26, Hôpital Fernand Widal, Paris, France and [c]Synt:em, Parc Scientifique Georges Besse, Nîmes, France.

Correspondence to J. Temsamani, Synt:em, Parc Scientifique Georges Besse, 30000 Nîmes, France.
Tel: +33 466 04 8666; fax: +33 466 04 8667;
e-mail: jtemsamani@syntem.com

Received 8 June 2004 **Revised form accepted** 29 July 2004

Introduction

Paclitaxel (PAX) has shown significant activity against human solid tumors, i.e. ovarian, head and neck, bladder, breast, and lung cancers [1,2]. Paclitaxel binds to and stabilizes microtubules, induces mitotic block at the metaphase/anaphase transition, and induces apoptosis [3–6]. The drug is administered i.v., but because of its limited aqueous solubility, PAX is formulated with polyethoxylated castor oil (Cremophor EL) in Taxol. One of the safety concerns associated with the clinical use of paclitaxel is the vehicle-based hypersensitivity reaction. The excipient Cremophor EL is believed to play a role in the hypersensitivity reactions occasionally observed in patients during paclitaxel therapy [7,8] and neurotoxicity [9]. The usefulness of paclitaxel in the preclinical and clinical settings is also limited by development of resistance, which appears to be mainly related to expression of tubulin isotypes and mutants [10–12] and/or overexpression of the P-glycoprotein (P-gp), a pump participating in the multidrug resistance (MDR) mechanisms [13,14]. P-gp is a 170-kDa ATP-dependent efflux pump, which functions as an ATP-driven pump capable of removing the drugs out of the cell membrane and consequently lowering the drug concentration inside the cell. Several *in vitro* studies have shown that co-treatment with P-gp inhibitors such as cyclosporin A, PSC833 or LY335979 results in reversal of paclitaxel resistance in P-gp-expressing cells [15–17] or *in vivo* [18,19].

PAX has also been used to treat malignant glioma and brain metastases [20–22]. However, brain tumors constitute a difficult problem, and the therapeutic benefit of paclitaxel has been variable and low. This could be attributed to its limited entry into the central nervous system (CNS). The blood–brain barrier (BBB), formed of endothelial cells, which express tight junctions and drug efflux transporters, is a major obstacle to developing effective treatments for CNS malignancies [23]. The brain capillary endothelium behaves like a continuous lipid bilayer and diffusion through this BBB is largely dependent on the lipid solubility of the drug [24]. Although paclitaxel is very lipophilic, concentrations in the CNS are very low after i.v. administration [25,26]. It is likely that the P-gp transporter contributes to its limited access to the brain. In fact, it has been demonstrated that P-gp and other ABC transporters are also present at the luminal side of the endothelial cells of the BBB [27–29]. As a consequence of P-gp expression at the BBB interface and overexpression within brain tumors, the bioavailability to brain tumor of paclitaxel is extremely limited, explaining in part the failure of brain tumor chemotherapy. An unsettled issue regarding P-gp and its direct significance to cancer treatment is whether the pump is able to reduce the penetration of anticancer agents into brain tumors. In contrast to brain capillaries, which constitute the BBB, brain tumors capillaries have been suggested to be 'leaky' [30]. However, a recent study by Gallo *et al.* [19] has shown that even in the neovasculature of brain tumors, P-gp has the facility to limit drug penetration at the level of the brain tumors capillaries, although somewhat less so than in normal brain.

Recently, we have shown that small peptide-vectors (SynB vectors) can enhance brain uptake of various

0959-4973

molecules including anticancer agents [31–34]. The potential of this approach as an effective delivery system for transporting drugs across the BBB has been demonstrated in a number of animal models [31–34]. The results obtained in these studies indicated that the use of peptide-vectors could enhance significantly the brain uptake of molecules without opening the tight junctions. We have also demonstrated that vectorization of doxorubicin by SynB vectors bypasses the P-gp, both *in vitro* and *in vivo* [35]. Thus vectorization of an anticancer agent known to be a P-gp substrate could be potentially beneficial at two levels for the treatment of brain tumors: higher influx through the BBB and better accumulation into tumor cells overexpressing P-gp. In the present study, we investigated the effect of vectorization of paclitaxel with SynB3 vector linked each other by a succinate linkage. We demonstrate that this peptide-vector enhances the solubility of paclitaxel and its brain uptake without affecting significantly its *in vitro* cytotoxicity. We also show that the conjugated paclitaxel bypasses the P-gp present at the BBB level.

Materials and methods

Materials

Cell lines

K562 (human erythroleukemia), 9L (rat glioma), SK-N-SH (human neuroblastoma) and MCF-7 (human breast carcinoma) cell lines were supplied by the ATCC (Rockville, MD). A2780 (human ovarian carcinoma) cell line was supplied by ECACC (Salisbury, UK). Raji (human Burkitt lymphoma), MDA-MB-231 and MDA-MB-435 (human breast carcinomas) and Lox (human melanoma) cells were provided by Professor Fodstad (Norwegian Radium Hospital, Oslo, Norway). All the cells were cultivated as recommended by the supplier. Culture medium (RPMI 1640, DMEM) purchased from Gibco (Cergy Pontoise, France) was supplemented with 10% heat-inactivated fetal calf serum (Gibco) and 1 mM HEPES. Incubations with free or vectorized paclitaxel were performed in culture medium exclusively composed of Opti-MEM (Gibco).

Animals

The P-gp-deficient (mdr1a$^{-/-}$, 30–40 g, 6–8 weeks old] and wild-type (mdr1a$^{+/+}$, 30–40 g, 6–8 weeks old) CF-1 mice were bred from genotyped mice provided by Charles River (Wilmington, MA). Animals were maintained under standard conditions of temperature and lighting, and had free access to food and water. The research adhered to the ethical rules of the French Ministry of Agriculture for experimentation with laboratory animals (law no. 87-848).

Synthesis

Peptide synthesis

SynB3 peptide was assembled by conventional solid-phase chemistry using a 9-fluorenylmethoxycarbonyl/tertiobutyl (Fmoc/tBu) protection scheme [36]. The crude peptide was purified on C_{18} preparative reverse-phase (RP)-HPLC after trifluoroacetic acid cleavage/deprotection. The purity of peptide was assessed by C_{18} reverse-phase analytic HPLC and MALDI-MS. The peptide sequence was SynB3 (RRLSYSRRRF, MW 1395 Da).

PAX-OSUC-SynB3 synthesis

PAX was linked to the SynB3 vector via the succinate linker in a one-pot two-steps reaction (Fig. 1). First, the PAX hemisuccinate is formed by reaction of the primary 2′-hydroxyl of PAX (1 eq.) with succinic anhydride (1 eq.) in the presence of catalytic amounts of diethylaminopyridine (DMAP, 0.1 eq.), in dimethylformamide (DMF) containing diisopropylethylamine (DIEA, 2–6 eq.). The progress of this first step is monitored by RP analytic HPLC.

In the second step, the peptide (1.3 eq.) dissolved in DMF is added to the reaction mixture, followed by the addition of the coupling agent PyBOP (1.2 eq.) dissolved in DMF. A further 2–4 eq. of DIEA are added to maintain an alkaline media. The progress of this second step is monitored by RP-HPLC and mass spectrometry. Finally, the conjugate is precipitated by addition of 10 volumes of diethylether, resuspended in H_2O/acetonitrile, purified by preparative RP-HPLC and then lyophilized. Purity was better than 95% as assessed by analytic RP-HPLC at 220 nm. MALDI-TOF spectrometry allowed us to confirm the molecular weight of the finished product.

[^{14}C]PAX-OSUC-SynB3 was synthesized using the same one-pot reaction strategy, starting from PAX [2-benzoyl ring-UL-^{14}C] (Sigma, l'Isle d'Abeau, France). The resulting product had a specific activity of 44.7 Ci/mol, and its radiochemical purity as assessed by HPLC liquid scintillation counting (Flo-One; Packard Instruments, Meriden, CA) was higher than 99%.

Cytotoxicity assay

Cytotoxicity of the compounds was assessed by the colorimetric MTT assay. Briefly, cells were seeded at 10^4 cells/well in a 96-well plate in Opti-MEM (Gibco) 24 h before the incubation. The cells were then incubated for 72 h with increasing concentrations of drugs. After this time, 0.5 mg/ml MTT (Sigma, St Quentin Fallavier, France) was added to each well and cells were incubated for another 4 h at 37°C. Medium was then removed, and cells and formazan crystals were solubilized in a DMF/SDS solution. Absorbance at 550 nm was determined by a Spectrafluor Plus Tecan plate reader. The EC_{50}, the drug concentration that decreases cell survival by 50% of maximal cell death compared with control (drug-free) cultures, was determined by plotting control absorbance

against log drug concentration. Each experiment was carried out in six copies and was repeated at least 3 times independently.

Cell cycle analysis

Cell cycle arrest in G_2/M induced by free and vectorized PAX was quantified by flow cytometry. Propidium iodide (PI), which binds DNA, provides a rapid and accurate means for quantifying both total nuclear DNA content and the fraction of cells in each phase of the cell cycle. The fluorescence signal intensity of the PI is directly proportional to the amount of DNA in each cell. K562 cells were seeded at 0.4×10^6 cells/ml in Optimem in 24-well plates. Cells were equilibrated at 37°C and 5% CO_2 for 2 h, prior to adding increasing concentrations of PAX or PAX-OSUC-SynB3 (as $\times 100$ solutions) for 24 h. Cells were stained with a PI (Sigma)-labeling solution (PBS containing 50 µg/ml PI, 0.1% Triton X-100 and 5% glycerol) before and after this 24 h incubation. Briefly, cell suspensions were diluted with PBS, centrifuged at 1200 r.p.m. for 5 min, resuspended in PI-labeling solution and then vortexed and incubated on ice in the dark for 20 min. Labeled cell suspensions were analyzed for DNA content on a FACSCalibur (Becton Dickinson, Mountain View, CA) flow cytometer ($\lambda_{emission} = 582 \pm 21$ nm). Flow cytometry was performed and analyzed on a Becton Dickinson flow cytometer using CellQuest software. EC_{50}s for cell cycle arrest in G_2/M were determined with GraphPad Prism software.

In situ mouse brain perfusion study

The *in situ* brain perfusion in P-gp-deficient mdr1a$^{-/-}$ and wild-type mice was carried out as described by Dagenais *et al.* [37]. Briefly, the right common carotid of ketamine/xylazine (i.p. 140/8 mg/kg) anesthetized mice was exposed. The right external carotid was ligated rostral to the occipital artery at the level of the bifurcation of the common carotid. The caudal side of the right common carotid was ligated and catheterized. The thorax was opened and the heart was cut before starting the perfusion. Brains were perfused for 60 s at a calibrated flow rate of 2.5 ml/min. The perfusion fluid consisted of a Krebs-bicarbonate buffer warmed at 37°C, and gassed with 95% O_2 and 5% CO_2 for pH control (7.4) containing either [^{14}C]PAX or [^{14}C]PAX-OSUC-SynB3 (0.2 µCi/ml) and [^{3}H]sucrose (0.6 µCi/ml). At the end of the perfusion time, the mouse was decapitated and total radioactivity in the brain was determined. PAX uptake was expressed as a single-time-point, unidirectional transfer constant (K_{in}; µl/s/g). Briefly, calculations were accomplished from the relationship $K_{in} = (Q_{tot} - V_v C_{pf})/(TC_{pf})$, where Q_{tot} is the measured quantity of [^{14}C]PAX in brain (vascular and extravascular) at the end of the experiments, V_v is the cerebral vascular volume, C_{pf} is the perfusion fluid concentration of [^{14}C]PAX and T is the perfusion time in seconds [38]. V_v was evaluated by the [^{3}H]sucrose space and calculated by the ratio between radioactivity of [^{3}H]sucrose (expressed in d.p.m. sucrose/g brain) and the perfusate sucrose concentration.

Statistical analysis

In vivo values were compared using a variance analysis (one way ANOVA) followed by an unpaired *t*-test. Values are expressed as mean ± SEM.

Calculation of logP values

The log*P* values were calculated using the software TSAR (Accelrys) using Ghose's Atomic approach [39].

Results

Enhanced solubility

Paclitaxel is known to have a very limited aqueous solubility and therefore is usually formulated with polyethoxylated castor oil (Cremophor EL). The solubility of paclitaxel in saline solution and water is less than 0.3 mg/l. When PAX was coupled to SynB3 (PAX-OSUC-SynB3) (Fig. 1), its solubility increased to more than 1 g/l. This increase in solubility was more than a 1000-fold on a molar basis compared with that of free paclitaxel.

In vitro cytotoxicity of free and vectorized paclitaxel

The *in vitro* cytotoxicity of PAX-OSUC-SynB3 was compared with that of free PAX on a series of cancer cell lines. The cells were incubated with the two compounds at various concentrations for 72 h and the cytotoxicity was measured using the MTT assay. The EC_{50}, defined as the drug concentration that decreases cell survival by 50% of maximal cell death compared with control (drug-free) cultures, is represented in Table 1.

Both free and vectorized paclitaxel showed a potent and dose-dependent growth-inhibitory effect against all the cell lines. The EC_{50} values for both compounds were almost similar for all the cell lines used except for the human breast carcinoma and neuroblastoma cell lines where a slight decrease in cytotoxicity was observed for PAX-OSUC-SynB3 (Table 1).

Cytotoxic mechanism of paclitaxel conjugate

To assess whether the mechanism of action of PAX-OSUC-SynB3 conjugate is the same as free paclitaxel, cell cycle analysis was performed in FACScan assay. The data show that PAX-OSUC-SynB3 arrests cells in G_2/M phase of the cell cycle, which is consistent with the mechanism of action of free PAX (Fig. 2A). At low concentration of both compounds, the main part of the cells was found at G_1 phase of the cell cycle. At higher concentrations, a complete shift from G_1 to G_2/M phase was observed. When the percentage of cells in G_2/M phase was plotted against the concentration, both free and vectorized PAX arrested the cell cycle in a concentration-dependent manner with a similar EC_{50} value (51.6 versus 66.8 nM, respectively) (Fig. 2B).

Fig. 1

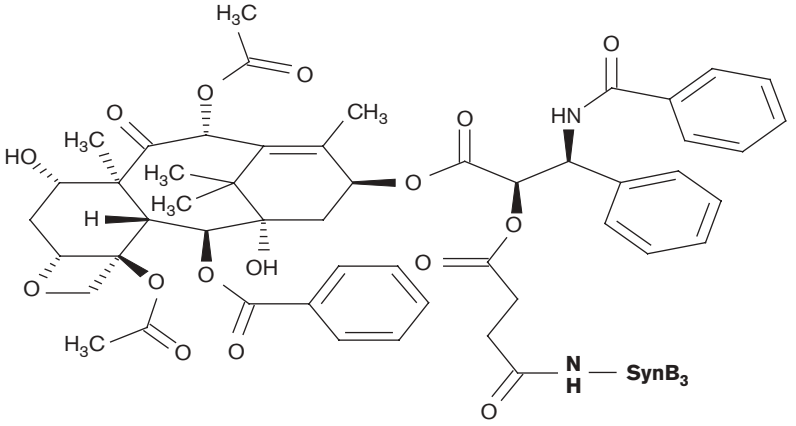

Structure of vectorized paclitaxel (PAX-OSUC-SynB3).

Table 1 Cytotoxic potency of free and vectorized paclitaxel in different cell lines

Cell line	Origin	EC_{50} (nM)	
		PAX	PAX-OSUC-SynB3
9L	Rat glioma	6.83 ± 2.6	4.98 ± 0.93
K562	Hu erythroleukemia	1.05 ± 0.28	1.68 ± 0.21
Raji	Hu Burkitt Lymphoma	2.92 ± 1.28	4.01 ± 1.61
MCF-7	Hu breast carcinoma	4.0 ± 0.59	20.0 ± 14.0
MDA-MB-231	Hu breast carcinoma	0.99 ± 0.06	3.81 ± 0.53
MDA-MB-435	Hu breast carcinoma	3.76 ± 1.0	16.47 ± 7.0
Lox	Hu melanoma	0.59 ± 0.26	1.23 ± 0.13
A2780	Hu ovarian carcinoma	0.76 ± 0.08	1.33 ± 0.38
SK-N-SH	Hu neuroblastoma	11.16 ± 0.52	68.11 ± 11.28

Data are the mean ± SEM of three to four independent experiments, each performed in sextuplets.

Enhanced brain uptake

We measured the brain uptake of free and vectorized PAX using the *in situ* brain perfusion in mice. To assess the integrity of the BBB, [^{3}H]sucrose was used as a marker of brain vascular volume since it does not measurably penetrate the BBB during brief periods (e.g. 60–120 s) of perfusion. When free or conjugated [^{14}C]PAX was perfused for 60 s, the distribution volume of [^{3}H]sucrose into the right cerebral hemisphere was between 13 and 19 µl/g, indicating that the permeability of the BBB has not been altered (data not shown). This is similar to the vascular volume values previously measured in our laboratory, which are typically about 20 µl/g [37]. This perfusion time (60 s) was chosen because it is short enough to limit risks of peptide or drug metabolism and high enough to measure reasonable quantities of radiolabeled PAX in brain tissues compared with the background noise of the detection method.

BBB permeabilities of free and vectorized PAX were then assessed (Fig. 3). The brain uptake of free PAX was very low after 60 s of perfusion ($K_{in} = 0.53 \pm 0.15$ µl/s/g). Interestingly, conjugation of paclitaxel to SynB3 significantly enhanced its brain uptake. The transport coefficient K_{in} measured for PAX-OSUC-SynB3 was 11.8 ± 2.5 µl/s/g.

Bypass of the P-gp at the BBB level

P-gp has been shown to be expressed in high levels in brain capillaries and is localized at the luminal surface of the endothelium [27,28]. It is therefore in the correct location to restrict permeation of a variety of drugs into the CNS. Recently, we have shown by an *in situ* mouse brain perfusion model that vectorized doxorubicin was able to bypass the P-gp present at the BBB level [35]. We therefore investigated whether the vectorized PAX is able to do so. We applied this *in situ* mouse brain perfusion method to evaluate the BBB penetration of free and vectorized PAX in both P-gp-deficient (mdr1a$^{-/-}$) and wild-type (mdr1a$^{+/+}$) mice. Mice were perfused with either [^{14}C]PAX or [^{14}C]PAX-OSUC-SynB3. K_{in} transport of PAX to the brain of wild-type mice was quite limited whereas a significant increase was observed in the mdr1a$^{-/-}$ CF-1 mice (0.45 ± 0.08 versus 1.25 ± 0.006, respectively) (Fig. 4). On the other hand, no differences of brain transport K_{in} of vectorized PAX were observed between the wild-type and mdr1a$^{-/-}$ mice (14.94 ± 1.94 versus 17.8 ± 1.015, respectively). These data suggest that contrary to free PAX; vectorized PAX is not recognized by the P-gp. As observed earlier, a significant enhancement of brain uptake, in wild type mice, was obtained for PAX-OSUC-SynB3 compared to free PAX.

Discussion

In this study we have coupled paclitaxel with SynB3 vector via a succinate linker in order to improve its brain uptake and chemical properties. SynB3 peptide

Fig. 2

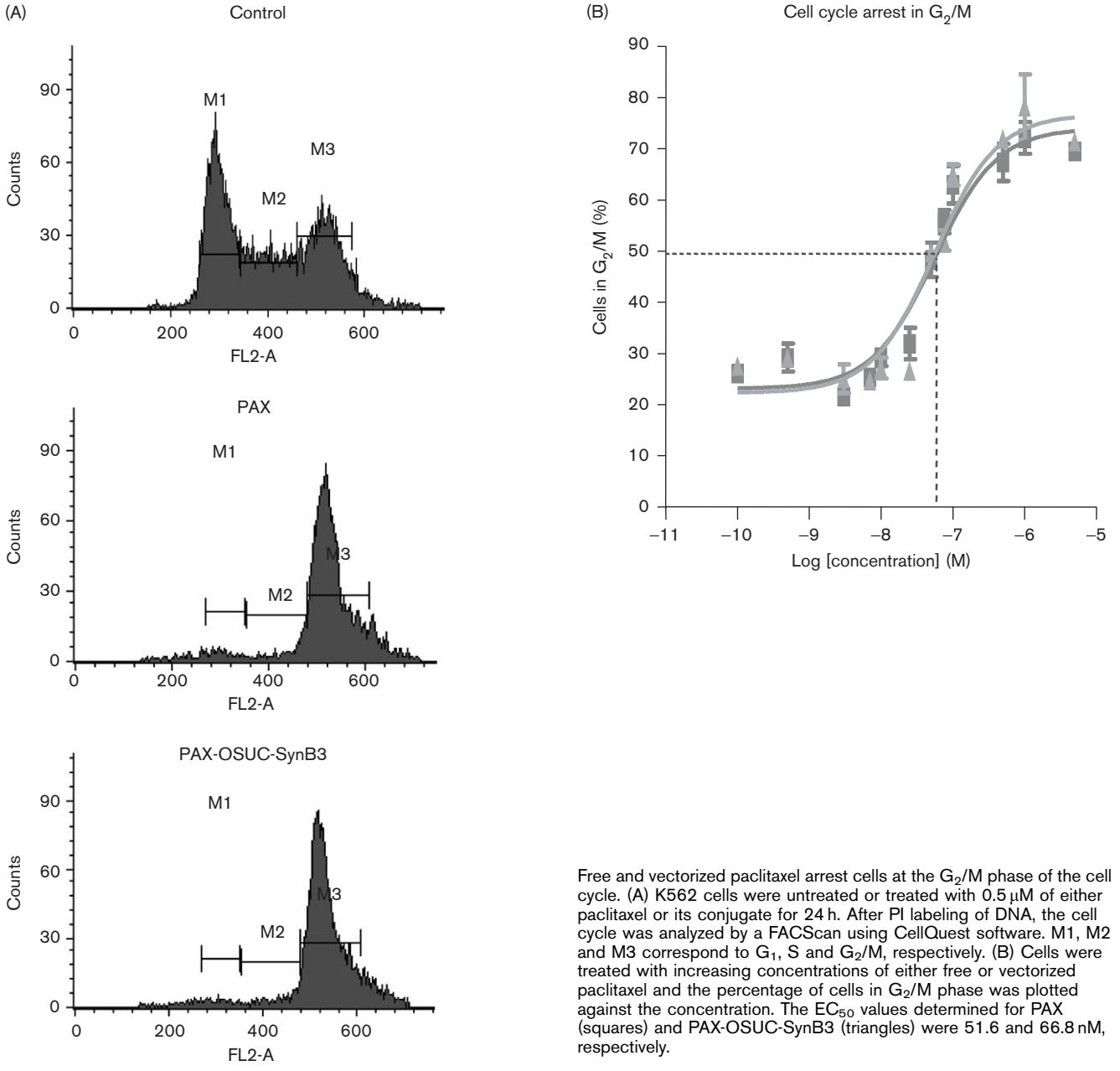

Free and vectorized paclitaxel arrest cells at the G_2/M phase of the cell cycle. (A) K562 cells were untreated or treated with 0.5 μM of either paclitaxel or its conjugate for 24 h. After PI labeling of DNA, the cell cycle was analyzed by a FACScan using CellQuest software. M1, M2 and M3 correspond to G_1, S and G_2/M, respectively. (B) Cells were treated with increasing concentrations of either free or vectorized paclitaxel and the percentage of cells in G_2/M phase was plotted against the concentration. The EC_{50} values determined for PAX (squares) and PAX-OSUC-SynB3 (triangles) were 51.6 and 66.8 nM, respectively.

(10 amino acids) has been shown to translocate efficiently through biological membranes including the BBB [32,34]. The present study demonstrates that coupling of paclitaxel with SynB3 enhances significantly its solubility. Paclitaxel is commercially available formulated with polyethoxylated castor oil (Cremophor EL). This excipient is believed to play a major role in the hypersensitivity reactions observed in patients while on paclitaxel therapy [7,8]. Therefore, using this peptide-vector strategy, large amounts of solubilizing agents such as Cremophor EL, polysorbate and ethanol are not required, so that side-effects typically associated with these solubilizing agents, such as anaphylaxis, hypotension and flushing, can be reduced.

We then evaluated the brain uptake of free and coupled paclitaxel using the *in situ* mouse brain perfusion method. This method is sensitive and allows the drug

concentration in the perfusion fluid to be controlled, avoiding confounding factors of systemic disposition such as the effect of metabolism [37]. Although paclitaxel is very lipophilic, after 60 s of brain perfusion, we only observed a low uptake of paclitaxel ($K_{in} = 0.53 \pm 0.2$ µl/g/s). This corroborates with studies showing that administration of paclitaxel by i.v. administration resulted in low concentrations in the CNS [25,26]. This low brain permeability could be explained by the efflux activity of P-gp at the BBB. Paclitaxel is actually transported by P-gp expressed at the brain capillaries in the physiological state [18,19,40]. To overcome MDR mechanisms, paclitaxel was given in combination with P-gp inhibitors [15–17,41]. However, if such drug combinations are effective *in vitro*, the high concentration of P-gp inhibitors necessary to overcome drug efflux limits their clinical application. Devising a successful method for a drug to bypass the BBB has the potential to transform an ineffective compound into an important advance in patient care.

Fig. 3

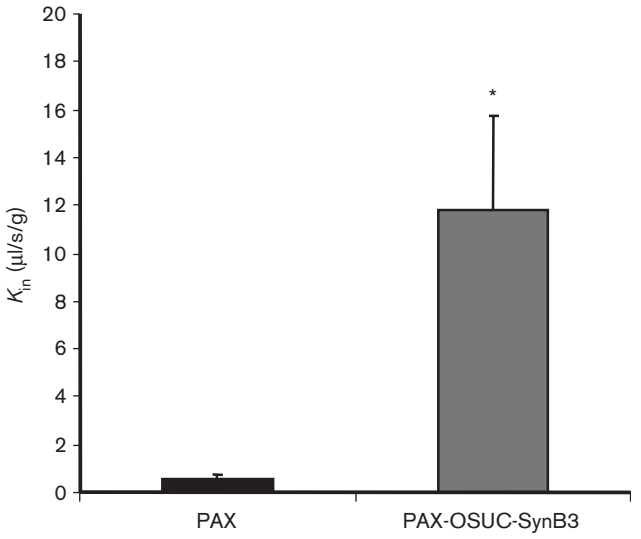

Brain transport coefficients (K_{in}) for [^{14}C]free and vectorized paclitaxel uptake in the right hemisphere of mouse rat brain after 60 s perfusion with buffer. The mice were perfused with 0.007 µmol/ml of PAX or 0.002 µmol/ml of PAX-OSUC-SynB3. Values are mean ± SEM ($n = 3–5$ animals). *$p < 0.05$.

By coupling paclitaxel to SynB3, we expected to increase its uptake in the brain and circumvent the efflux activity of P-gp. It is noteworthy that the coupling will make the compound less lipophilic (calculated log$P = 3.96$ for PAX and –5.53 for PAX-OSUC-SynB3), which in fact should reduce the permeability through the BBB. However, a significant 27-fold increase in paclitaxel brain uptake was obtained for the conjugated drug, compared to free paclitaxel (14.17 versus 0.53 µl/g/s). This increase in brain uptake obtained for the vectorized paclitaxel might be explained by the translocation properties of the SynB3 vector and also by the fact that vectorized paclitaxel is not recognized by the P-gp. This was furthermore confirmed by the experiment using P-gp-deficient mice. We observed that brain uptake of [^{14}C]PAX was increased in P-gp-deficient mice, confirming the recognition by the P-gp. Interestingly, [^{14}C]PAX-OSUC-SynB3 brain uptake in mdr1a$^{-/-}$ mice was identical to that observed in wild-type mice, suggesting that it bypasses the P-gp. A similar result was obtained when doxorubicin, another P-gp

Fig. 4

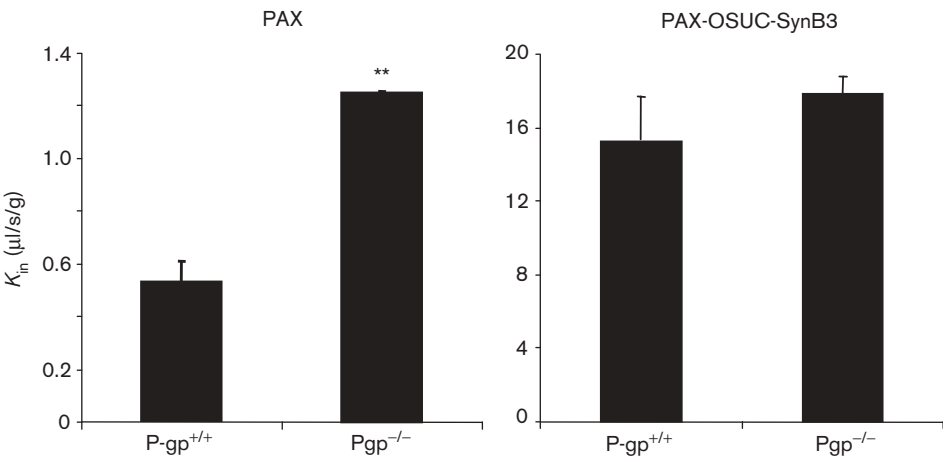

Brain transport coefficients (K_{in}) for [^{14}C]PAx and [^{14}C]PAX-OSUC-SynB3 uptake in the right hemisphere of wild-type and mdr1a$^{-/-}$ mice. Animals were perfused for 60 s with 0.005 µmol/ml of either paclitaxel of PAX-OSUC-SynB3. Each bar represents a mean ± SEM ($n = 2–3$ animals). ***$p < 0.001$.

substrate, was conjugated to SynB vectors [35]. All these results highlight a crucial difference between the mechanism of uptake of free and vectorized paclitaxel.

The mechanism by which vectorized paclitaxel enters the brain is not yet clear, but might involve adsorptive-mediated endocytosis, a mechanism reported for the vectorized doxorubicin with SynB3 [32]. SynB3 used in this study is positively charged (five positive charges), and this net positive charge is likely to play a major role in electrostatic interactions between the positive charges of the peptide vector and the negative surface charges of the endothelial cells composing the BBB [42]. We have shown that the brain uptake using SynB3 vector does not involve a chiral receptor since no difference in brain uptake could be seen between SynB vectors whose amino acids are in either the L- or the D-enantiomeric form [32,43]. We have also reported that the passage of SynB-conjugated drugs can be inhibited in a competitive manner by polycationic molecules such as poly(L-lysine) or protamine, which act as endocytosis inhibitors [32,43]. This kind of electrostatic interactions between cationic compound and negative charges of the endothelial cells suggest that the crossing of BBB by SynB vectors is via an energy-dependent adsorptive-mediated endocytosis mechanism as it was observed for other cationic peptides as ebiratide [44].

In this study, SynB3 was covalently linked to paclitaxel at the 2′-hydroxyl position. Coupling there has been shown to eliminate the microtubule assembly activity of paclitaxel [45,46]. By attaching SynB3 at the 2′-position on paclitaxel, we hoped to create an inactive prodrug that would require hydrolysis back to paclitaxel to be cytotoxic. Few lines of evidence support this. First, the *in vitro* studies showed that vectorized paclitaxel, like free paclitaxel, arrests cell cycle progression at the G_2/M phase of the cell cycle at 24 h and that the EC_{50} values obtained in the various tumor cell lines after a 72-h incubation are not significantly different. Since these studies are carried out for a long period of time (24 and 72 h), it is most likely that paclitaxel is released from the linker. The succinate linker is not a stable linker and can be susceptible to hydrolysis by esterases present inside the cells. We have performed some preliminary *in vitro* cytotoxicity experiments using a more stable linker (carbamate linker) and we have observed a significant loss of activity of the conjugate compared with that of free paclitaxel (C. Gros *et al.*, unpublished data). Second, the *in vitro* cytotoxicity studies in resistant cells (K562/ADR) showed that there was no bypass of the P-gp since a similar EC_{50} was obtained for free and vectorized paclitaxel (data not shown). This somewhat conflicting result with the one obtained with the *in situ* brain perfusion in P-gp-deficient mice might be explained by the fact that *in vitro* cytotoxicity studies are performed for 72 h and therefore the conjugate might be hydrolyzed by esterases and releasing free paclitaxel; while the *in situ* brain perfusion is carried out for a very short period of time (60–120 s) in which the conjugate is still intact. Taken together, these studies support the conclusion that vectorized paclitaxel must be converted to paclitaxel either intracellularly or in the vicinity of cells to be cytotoxic. Therefore, the use of this peptide-mediated strategy might serve as useful prodrugs of paclitaxel. Studies are ongoing to assess the effect of vectorization at other positions of paclitaxel (e.g. C-7).

Our results show that vectorization of paclitaxel enhances its solubility and brain delivery. We also show by the *in situ* brain perfusion in P-gp-deficient mice that vectorized paclitaxel bypasses the P-gp present at the luminal side of the BBB. Therefore, this study supports the usefulness of peptide-mediated strategies for improving the chemical properties and brain delivery of paclitaxel into the CNS. Toward this goal, future studies are ongoing to explore the anti-tumor potential of the conjugate *in vivo* in brain tumor models.

Acknowledgments

The excellent initial work of Dr C. Rousselle and M. Smirnova is gratefully acknowledged. We would like to thank Professor Fodstad for the cell lines, Christophe Lalanne for peptide synthesis, and Stéphanie Chancel, Sylvine Carrondo and Martine Mazel for help with cytotoxicity experiments. We are also indebted to Marc Adenot for Log*P* calculations and to C. Rebouissou, responsible of the FACS facilities at the Institut de Génétique Moléculaire de Montpellier.

References

1 Huizing MT, Misser VH, Pieters RC, Ten Bokkel Huinink WW, Veenhof CH, Vermorken JB, *et al.* Taxanes: a new class of antitumor agents. *Cancer Invest* 1995; **13**:381–404.
2 Rowinsky EK, Wright M, Monsarrat B, Lesser GJ, Donehower RC. Taxol: pharmacology, metabolism and clinical implications. *Cancer Surv* 1993; **17**:283–301.
3 Parness J, Horwitz SB. Taxol binds to polymerised tubulin *in vitro*. *J Cell Biol* 1981; **91**:479–487.
4 Manfreddi JJ, Parness J, Howitz SB. Taxol binds to cellular microtubules. *J Cell Biol* 1982; **94**:688–696.
5 Jordan MA, Toso RJ, Thrower D, Wilson L. Mechanism of mitotic block and inhibition of cell proliferation by taxol at low concentrations. *Proc Natl Acad Sci USA* 1993; **90**:9552–9556.
6 Derry WB, Wilson L, Jordan MA. Substoichiometric binding of taxol suppresses microtubules dynamics. *Biochemistry* 1995; **34**:2203–2211.
7 Weiss RB, Donehower RC, Wiernik PH, Ohnuma T, Gralla RJ, Trump DL, *et al.* Hypersensitivity reactions from taxol. *J Clin Oncol* 1990; **8**: 1263–1268.
8 Gelderblom H, Verweij J, Nooter K, Sparreboom A, Cremophor EL. The drawbacks and advantages of vehicle selection for drug formulation. *Eur J Cancer* 2001; **37**:1590–1598.
9 Onetto N, Canetta R, Winograd B, Catane R, Dougan M, Grechko J, *et al.* Overview of Taxol safety. *J Natl Cancer Inst Monogr* 1993; **15**:131–139.
10 Cabral F, Barlow SB. Mechanisms by which mammalian cells acquire resistance to drugs that affect microtubules assembly. *FASEB J* 1989; **3**:1593–1599.
11 Ohta S, Nishio K, Kubota N, Ohmori T, Funayama Y, Ohira T, *et al.* Characterization of a taxol-resistant human small-cell lung cancer cell line. *Jpn J Cancer Res* 1994; **85**:290–297.

12 Giannakakou P, Sackett DL, Kang YK, Zhan Z, Buters JT, Fojo T, *et al.* Paclitaxel-resistant human ovarian cancer cells have mutant beta-tubulins that exhibit impaired paclitaxel-driven polymerization. *J Biol Chem* 1997; **272**:17118–17125.

13 Gottesman MM, Pastan I. Biochemistry of multidrug resistance mediated by the multidrug transporter. *Annu Rev Biochem* 1993; **62**:385–427.

14 Bradley G, Ling V. P-glycoprotein, multidrug resistance and tumor progression. *Cancer Metastasis Rev* 1994; **13**:223–233.

15 Jachez B, Nordamin R, Loor F. Restoration of taxol sensitivity of multidrug-resistant cells by the cyclosporine SDZ PSC 833 and the cyclopeptide SDZ. *J Natl Cancer Inst* 1993; **85**:478–483.

16 Cardarelli CO, Aksentijerich I, Pastan I, Gottesman MM. Differential effects of P-glycoprotein inhibitors on NIH3T3 cells transfected with wild-type (G185) or mutant (V185) multidrug transporters. *Cancer Res* 1995; **55**:1086–1091.

17 Dantzig AH, Shepard RL, Cao J, Law KL, Ehlhardt WJ, Baughman TM, *et al.* Reversal of P-glycoprotein-mediated multidrug resistance by a potent cyclopropyldibenzosuberane modulator, LY335979. *Cancer Res* 1996; **56**:4171–4179.

18 Fellner S, Bauer B, Miller DS, Schaffrik M, Fankhanel M, *et al.* Transport of paclitaxel (Taxol) across the blood-brain barrier *in vitro* and *in vivo*. *J Clin Invest* 2002; **110**:1309–1318.

19 Gallo JM, Li S, Guo P, Reed K, Ma J. The effect of P-glycoprotein on paclitaxel brain and brain tumor distribution in mice. *Cancer Res* 2003; **63**:5114–5117.

20 Lee JS, Pisters KM, Komaki R, Glisson BS, Khuri FR, Schea R, *et al.* Paclitaxel/carboplatin chemotherapy as primary treatment of brain metastases in non-small cell lung cancer: a preliminary report. *Semin Oncol* 1997; **24**(**4 suppl 12**):S52–S55.

21 Glantz MJ, Chamberlain MC, Chang SM, Prados MD, Cole BF. The role of paclitaxel in the treatment of primary and metastatic brain tumors. *Semin Radiat Oncol* 1999; **9**:27–33.

22 Brandes AA, Pasetto LM, Monfardini S. New drugs in recurrent high grade gliomas. *Anticancer Res* 2000; **20**:1913–1920.

23 Blasberg RG, Groothuis DR. Chemotherapy of brain tumors: physiological and pharmacokinetics considerations. *Semin Oncol* 1986; **13**: 70–82.

24 Abbott NJ, Romero IS. Transporting therapeutics across the blood–brain barrier. *Mol Med Today* 1996; **2**:106–113.

25 Eiseman JL, Eddington ND, Leslie J, MacAuley C, Sentz DL, Zuhowski M, *et al.* Plasma pharmacokinetics and tissue distribution of paclitaxel in CD2F1 mice. *Cancer Chemother Pharmacol* 1994; **34**:465–471.

26 Heimans JJ, Vermorken JB, Wolbers JG, Eeltink CM, Meijer OW, Taphoorn MJ, *et al.* Paclitaxel (taxol) concentrations in brain tumor tissue. *Ann Oncol* 1994; **5**:951–953.

27 Cordon-Cardo C, O'Brien JP, Casals D, Rittman-Grauer L, Biedler JL, Melamed MR, *et al.* Multidrug-resistance gene (P-glycoprotein) is expressed by endothelial cells at blood–brain barrier sites. *Proc Natl Acad Sci USA* 1989; **86**:695–698.

28 Beaulieu E, Demure M, Whites L, Believe R. P-glycoprotein is strongly expressed in the luminal membranes of the endothelium of blood vessels in the brain. *Biochem J* 1997; **326**:539–544.

29 Cisternino S, Mercier C, Bourasset F, Roux F, Scherrmann JM. Expression, transport activity and up-regulation of the multidrug-resistance Abcg2/Bcrp1 at the mice blood-brain barrier. *Cancer Res* 2004; **64**:3296–3301.

30 Stewart DJ. A critique of the role of the blood–brain barrier in the chemotherapy of human brain tumors. *J Neuro-Oncol* 1994; **20**: 121–139.

31 Rousselle C, Clair P, Lefauconnier JM, Kaczorek M, Scherrmann JM, Temsamani J. New advances in the transport of doxorubicin through the blood–brain barrier by a peptide vector-mediated strategy. *Mol Pharmacol* 2000; **57**:679–686.

32 Rousselle C, Smirnova M, Clair P, Lefauconnier JM, Chavanieu A, Calas B, *et al.* Enhanced delivery of doxorubicin into brain via a peptide-vector mediated strategy: saturation kinetics and specificity. *J Pharmacol Exp Ther* 2001; **296**:124–131

33 Rousselle C, Clair P, Temsamani J, Scherrmann JM. Improved brain delivery of benzylpenicillin with a peptide-vector-mediated strategy. *J Drug Target* 2002; **10**:309–315.

34 Rousselle C, Clair P, Smirnova M, Kolesnikov Y, Pasternak GW, Gac-Breton S, *et al.* Improved brain uptake and pharmacological activity of dalargin using a peptide-vector-mediated strategy. *J Pharmacol Exp Ther* 2003; **306**: 371–376.

35 Mazel M, Clair P, Rousselle C, Vidal P, Scherrmann JM, Mathieu D, *et al.* Doxorubicin–peptide conjugates overcome multidrug resistance. *Anticancer Drugs* 2001; **12**:107–116.

36 Atherton E, Sheppard RC. Reaction procedures and operating techniques. In: Rockwood D, Hams BD (editors): *Solid Phase Peptide Synthesis: A Practical Approach*. Oxford: IRL Press; 1989, pp. 131–137.

37 Dagenais C, Rousselle C, Pollack GM, Scherrmann JM. Development of an *in situ* mouse brain perfusion model and its application to *mdr*1a P-glycoprotein-deficient mice. *J Cereb Blood Flow Metab* 2000*;* **20**:381–386.

38 Smith QR. Brain perfusion systems for studies of drug uptake and metabolism in the central nervous system. *Pharm Biotechnol* 1996; **8**: 285–307.

39 Ghose AK, Crippen GM. Atomic physicochemical parameters for three-dimensional structure directed quantitative structure–activity relationships I. partition coefficients as a measure of hydrophobicity. *J Comput Chem* 1986; **7**:565–577.

40 Rice A, Michaelis ML, Georg G, Liu Y, Turunen B, Audus KL. Overcoming the blood–brain barrier to taxane delivery for neurodegenerative diseases and brain tumors. *J Mol Neurosci* 2003; **20**:339–343.

41 Kemper EM, Cleypool C, Boogerd W, Beijnen JH, Van Tellingen O. The influence of the P-glycoprotein inhibitor zosuquidar trihydrochloride (LY335979) on the brain penetration of paclitaxel in mice. *Cancer Chemother Pharmacol* 2003; **53**:173–178.

42 Nagy Z, Peters H, Huttner I. Charge-related alterations of the cerebral endothelium. *Lab Invest* 1983; **49**:662–671.

43 Drin G, Cottin S, Blanc E, Rees AR, Temsamani J. Studies on the internalization mechanism of cationic cell-penetrating peptides. *J Biol Chem* 2003; **278**:31192–31201.

44 Terasaki T, Takakuwa S, Saheki A, Moritani S, Shimura T, Tabata S, Tsuji A. Adsorptive-mediated endocytosis of an adrenocorticotropic hormone (ACTH) analogu, ebiratide, into the blood–brain barrier: studies with monolayers of primary cultured bovine brain capillary endothelial cells. *Pharm Res* 1992; **9**:529–534.

45 Mellado W. Preparation and biological activity of Taxol acetates. *Biochem Biophys Res Commun* 1984; **124**:329–336.

46 Kingston DG. Taxol: the chemistry and structure–activity relationships of a novel anticancer agent. *Trends Biotechnol* 1994; **12**:222–227.